arXiv:1303.2612v1 [astro-ph.HE] 11 Mar 2013

Quasi-Thermal Neutrinos from Rotating Proto-Neutron Stars

Kohta Murase[1,3], Basudeb Dasgupta[2,3], and Todd A. Thompson[3,4]
[1]*Hubble Fellow — Institute for Advanced Study, Princeton, New Jersey 08540, USA*
[2]*International Centre for Theoretical Physics, Trieste 34014, Italy*
[3]*CCAPP, The Ohio State University, Columbus, Ohio 43210, USA*
[4]*Department of Astronomy, The Ohio State University, Columbus, Ohio 43210, USA*

(Dated: 12 March 2013)

Rotating and magnetized proto-neutron stars (PNSs) may have neutron-loaded relativistic winds. These neutrons should cause inelastic collisions in the stellar material or around the termination shock, producing $\sim 0.1-1$ GeV neutrinos, without relying on cosmic-ray acceleration mechanisms. We show that PINGU and Hyper-Kamiokande can detect such neutrinos from nearby supernovae, by reducing the atmospheric neutrino background via coincident detection of MeV neutrinos or gravitational waves and optical follow-up observations. Detection of these quasi-thermal neutrinos would provide important clues to the physics of magnetic acceleration, nucleosynthesis, the relation between supernovae and gamma-ray bursts, and the properties of newly born neutron stars.

PACS numbers: 95.85.Ry, 97.60.Bw, 98.70.Rz

Proto-neutron stars (PNSs) are produced in core-collapse supernovae (SNe), and cool via radiation of MeV neutrinos on a timescale of $\sim 10-100$ s [e.g., 1, 2]. A fraction of these thermal neutrinos deposit their energy in the PNS atmosphere, driving a wind with mass loss rate $\dot{M}$ that injects energy into the shocked stellar material and forms a wind-driven bubble in the SN cavity [e.g., 3]. For non-rotating and non-magnetic PNSs, the wind kinetic energy is tiny compared to the SN explosion energy, and the wind is non-relativistic throughout the cooling epoch [e.g., 4]. However, if PNSs are rotating and magnetized, they transition from non-relativistic and thermally-driven to relativistic and Poynting-dominated [e.g., 5, 6]. The magnetization of the flow is [5, 6, 13]

$$\sigma \approx \frac{B_{\rm dip}^2 R_{\rm ns}^4 \Omega^2}{\dot{M} c^3} f_{\rm op}^2, \tag{1}$$

where $R_{\rm ns}$ is the PNS radius, $B_{\rm dip}$ is the surface dipolar field strength, Ω is the angular frequency of the PNS, and $f_{\rm op}$ takes into account that the outflow comes from only the open fraction of the PNS surface. The transition from non-relativistic to relativistic occurs at $\sigma \sim 1$ where the Alfvén speed becomes $\sim c$ as $\dot{M}$ decreases.

Rapidly rotating and/or strongly magnetized PNSs may be related to various explosion phenomena. Estimates suggest that $\gtrsim 10\%$ of SNe lead to magnetars with $B_{\rm dip} \sim 10^{14-15}$ G [7], which may be generated by rapid rotation via the dynamo mechanism [8]. Rotation and/or magnetization may also modify the explosion dynamics. If the wind power exceeds $\sim 10^{48}$ erg s^{-1}, the wind can be collimated [9, 10], and these jets may lead to gamma-ray bursts (GRBs) [5, 6, 11]. If the rotation rate or magnetic field strength is not sufficiently high, a quasi-spherical wind or a pair of choked jets hidden by the stellar material may result, potentially leading to hypernovae and super-luminous SNe [5, 6, 12].

Neutrons are loaded in the PNS wind by neutrino heating, and they may also be important for synthesis of nuclei [14]. We show that relativistic neutrons are produced by magnetic acceleration of the flow as σ becomes $\gg 1$, and that $\sim 0.1-1$ GeV neutrinos should be generated via the np reaction. These neutrinos can be detected by planned facilities such as PINGU [15] and Hyper-Kamiokande (HK) [16], and their characterization would allow us to probe the physics of PNSs, the early wind/jet dynamics, and magnetic acceleration in an environment inaccessible to photons. Throughout this work, we use $Q_x \equiv Q/10^x$ in CGS units unless otherwise specified.

Relativistic PNS winds.— Mass-loss occurs during the PNS cooling phase by neutrino heating, mainly via $\nu_e n \rightleftharpoons e^- p$ and $\bar{\nu}_e p \rightleftharpoons e^+ n$. In unmagnetized winds [4, 6]

$$\begin{aligned} \dot{M}_\nu &\approx 1.4 \times 10^{-4} M_\odot \text{ s}^{-1} L_{\nu,52}^{5/3} (\varepsilon_\nu/15 \text{ MeV})^{10/3} \\ &\times (1+\epsilon_{\rm es})^{5/3} R_{\rm ns,6}^{5/3} (M_{\rm ns}/1.4\, M_\odot)^{-2}, \end{aligned} \tag{2}$$

where L_ν is the neutrino ($\nu_e + \bar{\nu}_e$) luminosity and ε_ν is the typical neutrino energy, which can be affected by rotation and magnetization [17]. Additional heating due to inelastic electron scattering gives a correction $f_{\rm es} \equiv 1 + \epsilon_{\rm es}$. The mass-loss rate is reduced by $f_{\rm op}$, while enhanced by $f_{\rm cen}$ due to the centrifugal force [18]. We describe the baryon mass-loss rate by $\dot{M}_b \approx \dot{M} = \dot{M}_\nu f_{\rm op} f_{\rm cen}$ [6]. By setting $\sigma \sim 1$ in Eq. (1), we find that the transition to relativistic flow occurs when $\dot{M}_b \approx \dot{M}_{\rm tr} \simeq 7.4 \times 10^{-6} M_\odot$ s^{-1} $B_{\rm dip,15}^2 P_{-2}^{-2} f_{\rm op}^2 R_{\rm ns,6}^4$, where $P = 2\pi/\Omega$.

The neutrino luminosity decreases gradually as a power law, until the PNS becomes transparent to neutrinos [2, 6]. Once $t_{\rm thin} \sim 10-100$ s, L_ν, ε_ν and $\dot{M}_\nu$ should decline rapidly. Eventually, $\dot{M}$ cannot be described by neutrino heating but by the Goldreich-Julian density $\dot{M}_{\rm GJ} \approx 2.5 \times 10^{-17} M_\odot$ s^{-1} $\mu_{\pm,6} B_{\rm dip,15} P_{-2}^{-2} R_{\rm ns,6}^3$ [19], where $\mu_\pm$ is the pair-multiplicity. Note that $\dot{M}_b = \dot{M}_{\rm GJ} m_p/(\mu_\pm m_e Y_e)$, where Y_e is the electron fraction.

For the purpose of simple estimates, we hereafter assume $M_{\rm ns} = 1.4 M_\odot$, $R_{\rm ns} = 10^6$ cm, $L_\nu \propto t^{-1} e^{-t/t_{\rm thin}}$,

$\varepsilon_\nu \propto L_\nu^{1/4}$ [2, 6]. Then, the transition time $t_{\rm tr}$, when the PNS wind becomes relativistic ($\sigma \sim 1$) is

$$\begin{aligned} t_{\rm tr} &\sim 3.2\ {\rm s}\ B_{\rm dip,15}^{-4/5} P_{-2}^{4/5} f_{\rm op}^{-2/5} f_{\rm cen}^{2/5} \\ &\times L_{\nu 0,52}^{2/3} (\varepsilon_{\nu 0}/15\ {\rm MeV})^{4/3} f_{\rm es}^{2/3}, \end{aligned} \quad (3)$$

where $L_{\nu 0}$ and $\varepsilon_{\nu 0}$ are defined at 1 s. Therefore, if magnetic fields are strong and/or rotation is rapid, the PNS wind becomes relativistic at $t \ll t_{\rm thin}$. If not, it will become so at $\sim t_{\rm thin}$ as $\dot{M}$ rapidly declines.

The σ parameter at $t_{\rm thin}$ is

$$\begin{aligned} \sigma(t_{\rm thin}) &\sim 1100 B_{\rm dip,15}^2 P_{-2}^{-2} f_{\rm op,-1} f_{\rm cen}^{-1} L_{\nu 0,52}^{-5/3} \\ &\times (\varepsilon_{\nu 0}/15\ {\rm MeV})^{-10/3} f_{\rm es}^{-5/3}, \end{aligned} \quad (4)$$

and $\dot{M}(t_{\rm thin}) \sim 6.5 \times 10^{-11}\ M_\odot\ {\rm s}^{-1}\ f_{\rm op,-1} f_{\rm cen} L_{\nu 0,52}^{5/3}$ $(\varepsilon_{\nu 0}/15\ {\rm MeV})^{10/3} f_{\rm es}^{5/3}$ for $t_{\rm thin} = 50$ s. We focus on the epoch $t \lesssim t_{\rm thin}$, since the flux of relativistic neutrons producing quasi-thermal neutrinos decreases strongly for $t \gg t_{\rm thin}$ even though the wind becomes more relativistic.

Wind acceleration.— At $t \gtrsim t_{\rm tr}$, the PNS wind is magnetically accelerated. It is known that magnetic energy is not efficiently converted to kinetic energy in ideal MHD [20]. However, efficient acceleration is required to explain jets of GRBs and active galaxies, and may be achieved by time-dependence or magnetic dissipation [see a review 21, and references therein]. When the maximum Lorentz factor $\Gamma_{\rm max} \approx \sigma$ is achieved at the saturation radius $R_{\rm sat} \approx R_{\rm mag}$, we can parametrize $\Gamma(r)$ as [22]

$$\Gamma(r) \approx \sigma \left(\frac{r}{R_{\rm mag}} \right)^{1/3}, \quad (5)$$

where $R_{\rm mag} \approx \pi c \sigma^2/(3\epsilon_{\rm rec}\Omega) \simeq 5.0 \times 10^{15}$ cm $\sigma_3^2 P_{-2} \epsilon_{\rm rec,-2}^{-1}$ [6, 22], and $\epsilon_{\rm rec}$ is a parameter characterizing magnetic reconnection [22, 23]. Note that more efficient dissipation or radiative acceleration leads to indices larger than 1/3 and smaller $R_{\rm sat}$. Hence, our results below are relatively conservative.

In our case, the wind/jet-driven bubble terminates at the reverse shock caused by the interaction between the flow and shocked/pre-shocked stellar material, which may be nearly-spherical or biconical [9, 24]. When the wind radius R_w is smaller than $R_{\rm mag}$, the final Γ is

$$\Gamma(R_w) \simeq 13 \sigma_3^{1/3} P_{-2}^{-1/3} \epsilon_{\rm rec,-2}^{1/3} R_{w,10}^{1/3}. \quad (6)$$

The maximum Lorentz factor is achieved only if there is no boundary to the flow (e.g., high wind power and successful jets) [9, 10] or acceleration is much faster (e.g., choked jets in the fireball scenario for GRBs).

Neutrons and ions have the same outflow velocity as long as they are coupled with $< \sigma_{\rm el} v > \approx \sigma_{np} c$ [25]. Here $\sigma_{\rm el}$ is the elastic cross section and $\sigma_{np} \approx 3 \times 10^{-26}\ {\rm cm}^2$ is the inelastic cross section. However, if the neutrons are decoupled during the flow acceleration, then they will have smaller Lorentz factor than the ions. Using the nucleon density $n_w = \dot{M}_b/(4\pi r^2 c m_p)$ and Eq. (5), $\tau_{np} \approx 0.5 n_w \sigma_{np} (R_{\rm dec}/\Gamma) = 1$ gives the decoupling radius

$$R_{\rm dec} \simeq 6.8 \times 10^8\ {\rm cm}\ \sigma_3^{-1} B_{\rm dip,15}^{3/2} P_{-2}^{-5/4} f_{\rm op,-1}^{3/2} \epsilon_{\rm rec,-2}^{-1/4}. \quad (7)$$

For $R_{\rm dec} < R_w, R_{\rm mag}$, the neutron Lorentz factor Γ_n is

$$\Gamma(R_{\rm dec}) \approx 5.1 B_{\rm dip,15}^{1/2} P_{-2}^{-3/4} f_{\rm op,-1}^{1/2} \epsilon_{\rm rec,-2}^{1/4}. \quad (8)$$

Because $R_{\rm mag} \propto \sigma^2$, it should increase rapidly in time (Eqs. 1 and 2). R_w also increases, but more slowly. Hence, if $R_{\rm mag}(t_{\rm tr}) < R_w(t_{\rm tr})$ at $t_{\rm tr}$, then $R_{\rm mag}$ eventually overtakes R_w. On the other hand, $R_{\rm dec}$ decreases with time, so it crosses $R_{\rm mag}$ and R_w as long as $R_{\rm dec}(t_{\rm tr})$ is large enough (that is satisfied in our cases). We define t_a by $R_{\rm dec}(t_a) = R_{\rm mag}(t_a)$ and t_b by $R_{\rm dec}(t_b) = R_w(t_b)$, respectively (see Fig. 1). (Note that $t_a \lesssim t_{\rm thin}$ and $t_b \lesssim t_{\rm thin}$ since σ abruptly increases around $t_{\rm thin}$.)

Neutrons and ions achieve the same final Lorentz factor in the early phase ($t < \max[t_a, t_b]$), whereas neutrons have lower final Lorentz factor in the later phase because of decoupling. If $t_a < t_b$, we have $\Gamma_n \approx \Gamma(R_w)$ at $t < t_b$ and $\Gamma_n \approx \Gamma(R_{\rm dec})$ at $t_b < t$. If $t_b < t_a$, we obtain $\Gamma_n \approx \Gamma(R_{\rm mag})$ at $t < t_a$ and $\Gamma_n \approx \Gamma(R_{\rm dec})$ at $t_a < t$. If $t_a \ll t_{\rm thin}$, we have

$$\begin{aligned} t_a &\sim 16\ {\rm s}\ B_{\rm dip,15}^{-3/5} P_{-2}^{1/2} f_{\rm op,-1}^{-1/5} f_{\rm cen}^{2/5} \epsilon_{\rm rec,-2}^{1/10} \\ &\times L_{\nu 0,52}^{2/3} (\varepsilon_{\nu 0}/15\ {\rm MeV})^{4/3} f_{\rm es}^{2/3}, \end{aligned} \quad (9)$$

using Eqs. (1) and (2). If $t_b \ll t_{\rm thin}$, assuming the typical velocity $V \approx R_w/t$, t_b is estimated to be

$$\begin{aligned} t_b &\sim 40\ {\rm s}\ B_{\rm dip,15}^{-1/7} P_{-2}^{3/14} f_{\rm op,-1}^{1/7} f_{\rm cen}^{2/7} \epsilon_{\rm rec,-2}^{-1/14} \\ &\times L_{\nu 0,52}^{10/21} (\varepsilon_{\nu 0}/15\ {\rm MeV})^{20/21} f_{\rm es}^{10/21} V_{8.5}^{-2/7}. \end{aligned} \quad (10)$$

Neutrons decay with proper lifetime of 886.7 s, so the decay radius $R_\beta \approx 2.7 \times 10^{14}$ cm $\Gamma_{n,1}$ is much longer than $R_{\rm dec}$, $R_{\rm mag}$ and R_w, in which we are interested.

Neutrons from disintegrated nuclei.— Neutrons may be produced around R_w via disintegration of nuclei, as well as those not used up in nucleosynthesis. Fe-group elements are mainly created if $Y_{e0} \gtrsim 0.5$, while the neutron capture channel is dominant and $A > 56$ nuclei are synthesized if $Y_{e0} \lesssim 0.5$. They could be seeds of ultra-high-energy cosmic rays (UHECRs) if they could survive (e.g., after successful jets break out) [14].

Nuclei may be spalled, which is relevant at $R_w \lesssim R_{\rm dec}$ since shocked nuclei collide with neutrons. They can also be disintegrated by photons mainly via the giant-dipole resonance $A\gamma \rightarrow A'N$ if $2\Gamma\varepsilon \geq 8.5$ MeV $(A/56)^{-1/6}$, where ε is the target photon energy in the stellar frame [26]. The wind/jet-driven bubble may be filled with photons provided by the SN explosion, since the SN shock or radioactive nuclei provide x and/or

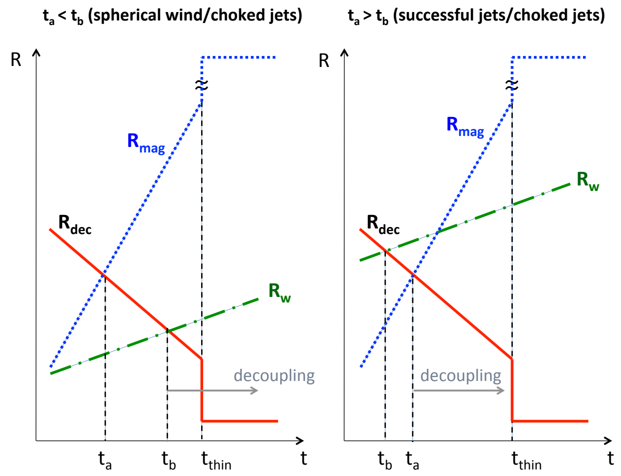
$t_a < t_b$ (spherical wind/choked jets)
$t_a > t_b$ (successful jets/choked jets)
R
R_{mag}
R_{dec}
R_w
decoupling
t_a
t_b
t_{thin}
t

FIG. 1: Schematic picture of $R_{\rm mag} \propto \sigma^2$, $R_{\rm dec} \propto \sigma^{-1}$ and $R_w \propto t^{1+\chi}$.

gamma rays, cascading down to optical photons as a result of thermalization. The SN temperature of ≈ 11 keV $\mathcal{E}_{\rm ph,49}^{1/4} R_{w,10}^{-3/4}$ allows nuclei to survive. However, disintegration can be caused by high-energy photons that are generated via shock dissipation or magnetic reconnection. We here consider effects of high-energy electrons produced around R_w. The PNS wind is Poynting-dominated after $t_{\rm tr}$, and the magnetic field is $B \sim 2.1 \times 10^8$ G $B_{\rm dip,15} P_{-2}^{-1} f_{\rm op,-1} R_{w,10}^{-1}$ from the shock-jump conditions. The reverse shock is hydrodynamically weak since the thermal energy in the downstream is much smaller than the magnetic energy, but small dissipation can be enough. The random energy per particle is $0.75\Gamma m_p c^2$ when ions are mainly protons, and the injection Lorentz factor of electrons is $\gamma_{e,i} \approx 0.75\epsilon_e \Gamma (m_p/m_e) Y_e^{-1}$. The characteristic synchrotron energy is $\varepsilon_{\rm syn} \sim 4.6$ MeV $\epsilon_{e,-1}^2 Y_e^{-2} \Gamma_1^2 B_{\rm dip,15} P_{-2}^{-1} f_{\rm op,-1} R_{w,10}^{-1} \gtrsim m_e c^2$, so synchrotron cascades will be developed and nuclei typically interact with boosted $\sim m_e c^2$ photons. Then, using $\kappa_A \sigma_{A\gamma} \approx 1.4 \times 10^{-27}$ cm^2 $(A/56)^{1/6}$ [26], the photodisintegration efficiency, $f_{A\gamma} \sim \kappa_A \sigma_{A\gamma} (\Gamma n_\gamma)(R_w/\Gamma^3)$, is

$$f_{A\gamma} \sim 3 (A/56)^{1/6} Y_e \Gamma_1^{-1} \sigma_3^{-1} B_{\rm dip,15}^{3/2} P_{-2}^{-3/2} f_{\rm op,-1}^{3/2} R_{w,10}^{-1/2} \quad (11)$$

Note that the Thomson opacity is $\tau_T \approx n_e \sigma_T (R_w/\Gamma) \simeq 0.66 Y_e \Gamma_1^{-1} R_{w,10}^{-1} (\dot{M}_b / 10^{-10.5}\ M_\odot\ {\rm s}^{-1}) \lesssim$ a few, so particles may be accelerated and high-energy photons can reach the upstream before they are thermalized.

Eq. (11) suggests that synchrotron photons can disintegrate nuclei and supply neutrons with $\Gamma \approx \min[\Gamma(R_w), \Gamma(R_{\rm mag})]$, giving an additional contribution of neutrinos. Hence, the fraction of neutrons (X_n) depends on outflow dynamics as well as the initial entropy and the initial electron fraction Y_{e0}. Note that $f_{A\gamma}$ declines with time, and nuclei would survive at $t \gg t_{\rm thin}$.

Neutrino production.— While the wind/jet excavates the stellar material, ions are quickly decelerated at the shock via radiation or collisionless processes. On the other hand, relativistic neutrons should be decelerated via np collisions, leading to neutrino production. Note that their deceleration scale $\sim 1/(n_w 0.5 \sigma_{np})$ is longer than $\sim 1/(n_e \sigma_T)$ and any relevant plasma scales. Even above $R_{\rm dec}$, the neutron beam goes through the shocked wind, but it is damped by the stellar material (with mass $M_{\rm sn}$). Neutrons leaving the flow are depleted until the SN ejecta reaches the pionosphere at $\approx 6.5 \times 10^{15}$ cm $(M_{\rm sn}/10 M_\odot)^{1/2}$.

Half of the neutron kinetic energy goes to neutrinos, so quasi-thermal neutrinos have a luminosity of

$$\mathcal{L}_\nu \approx 0.5 (\Gamma_n - 1) X_n \dot{M}_b c^2. \quad (12)$$

For $t_a < t_b$, assuming $V \propto t^\chi$ with small χ, we have $\mathcal{L}_\nu \propto t^{-(4-\chi)/3}$ until t_b, so $\mathcal{L}_\nu$ and $\mathcal{E}_\nu$ typically decreases as time. Inelastic collisions occur only when $\Gamma_n \geq 1.37$, almost after the PNS wind becomes relativistic at $\sim t_{\rm tr}$. (Of course, both R_w and $R_{\rm mag}$ have to be larger than $R_{\rm lc} \equiv c/\Omega$.) Hence, the total energy of neutrinos is $\mathcal{E}_\nu \sim 0.5 X_n (0.37 \dot{M}_b)|_{t_{\rm tr}} c^2 t_{\rm tr}$, and we have

$$\begin{aligned} \mathcal{E}_\nu^{\rm iso} &\sim 7.8 \times 10^{48}\ {\rm erg}\ X_n B_{\rm dip,15}^{6/5} P_{-2}^{-6/5} f_{\rm op}^{8/5} f_{\rm cen}^{2/5} \\ &\times L_{\nu 0,52}^{2/3} (\varepsilon_{\nu 0}/15\ {\rm MeV})^{4/3} f_{\rm es}^{2/3} f_b^{-1}, \end{aligned} \quad (13)$$

where f_b is the beaming factor and the typical neutrino energy is $E_\nu \approx 0.25 m_\pi c^2 \simeq 35$ MeV. If the PNS wind is collimated as in GRB jets, the observed fluence is enhanced by $f_b^{-1} \sim 100$, where such neutrinos could be seen as a tail by water-Cherenkov neutrino telescopes such as Super-Kamiokande and a next-generation detector HK.

Since Γ_n increases with time, higher-energy neutrinos are produced later, and these are more easily detected. However, L_ν and $\mathcal{L}_\nu$ decline abruptly after $t_{\rm thin}$. For neutrinos originating from intrinsic neutrons, the highest-energy contribution is generated at $\sim t_b$, at which we have $\mathcal{E}_\nu \sim 0.5 X_n (\Gamma_n \dot{M}_b)|_{t_b} c^2 t_b$ and Eq. (10) leads to

$$\begin{aligned} \mathcal{E}_\nu^{\rm iso} &\sim 2.5 \times 10^{47}\ {\rm erg}\ X_n B_{\rm dip,15}^{5/7} P_{-2}^{-15/14} f_{\rm op,-1}^{9/7} f_{\rm cen}^{4/7} \epsilon_{\rm rec,-2}^{5/14} \\ &\times L_{\nu 0,52}^{20/21} (\varepsilon_{\nu 0}/15\ {\rm MeV})^{40/21} f_{\rm es}^{20/21} V_{8.5}^{3/7} f_b^{-1}. \end{aligned} \quad (14)$$

Though Eq. (14) is valid for neutrons produced via photodisintegration of nuclei, they achieve higher Lorentz factors at $t \gtrsim t_b$ and their contribution at $\sim t_{\rm thin}$ is still significant. Using $\mathcal{E}_\nu \sim 0.5 X_n (\Gamma(R_w) \dot{M}_b)|_{t_{\rm thin}} c^2 t_{\rm thin}$,

$$\begin{aligned} \mathcal{E}_\nu^{\rm iso} &\sim 3.8 \times 10^{46}\ {\rm erg}\ X_n B_{\rm dip,15}^{2/3} P_{-2}^{-1} f_{\rm op,-1}^{4/3} f_{\rm cen}^{2/3} \epsilon_{\rm rec,-2}^{1/3} \\ &\times L_{\nu 0,52}^{10/9} (\varepsilon_{\nu 0}/15\ {\rm MeV})^{20/9} f_{\rm es}^{10/9} R_{w,10}^{1/3} f_b^{-1}, \end{aligned} \quad (15)$$

is obtained for this case (where $t_{\rm thin} = 50$ s is used).

For $t_b < t_a$, $\mathcal{L}_\nu \propto \Gamma_n \dot{M}_b \propto t^0$ until t_a and Γ_n saturates when $R_{\rm mag} = R_{\rm dec}$. Then, for both the origins of neutrons, we have $\mathcal{E}_\nu \sim 0.5 X_n (\Gamma_n \dot{M}_b)|_{t_a} c^2 t_a$ and

$$\begin{aligned} \mathcal{E}_\nu^{\rm iso} &\sim 1.0 \times 10^{48}\ {\rm erg}\ X_n B_{\rm dip,15}^{7/5} P_{-2}^{-3/2} f_{\rm op,-1}^{9/5} f_{\rm cen}^{2/5} \epsilon_{\rm rec,-2}^{1/10} \\ &\times L_{\nu 0,52}^{2/3} (\varepsilon_{\nu 0}/15\ {\rm MeV})^{4/3} f_{\rm es}^{2/3} f_b^{-1}. \end{aligned} \quad (16)$$

In either of Eqs. (14)-(16), the neutrino spectrum may extend to $\sim \Gamma_{n,1}$ GeV with the typical energy $E_\nu \approx 0.05\Gamma_n m_n c^2 \simeq 0.47$ GeV $\Gamma_{n,1}$ for $\Gamma_n \gg 1$ [31]. Such GeV neutrinos are good targets for PINGU, a planned low-energy extension of IceCube, as well as HK.

In the standard pulsar phase ($t \gg t_{\rm thin}$), $\dot{M} \approx \dot{M}_{\rm GJ}$ and we do not expect intrinsic neutrons. The wind will be dominated by electron-positron pairs, though nuclei may be stripped from the surface. Neutrons may be supplied by photodisintegration. However, since the ambient photon density is already low, photodisintegration and neutrino production are likely to be inefficient.

Neutrino detection.— From Eqs. (13)-(16), the energy fluence of quasi-thermal neutrinos per flavor is $E_\nu^2 \phi_\nu \simeq 28~{\rm erg~cm^{-2}}~\mathcal{E}_{\nu,48}^{\rm iso}(D/10~{\rm kpc})^{-2}$.

PINGU has sensitivity to $1-10$ GeV neutrinos with an effective area of $\sim 4\times10^{-3}~{\rm cm}^2$ for $\nu_e+\bar{\nu}_e$ and $\sim 2\times10^{-3}~{\rm cm}^2$ for $\nu_\mu+\bar{\nu}_\mu$, respectively, at ~ 1 GeV. So, $\sim 100~\mathcal{E}_{\nu,48}^{\rm iso}$ events are expected for a SN at 10 kpc. In the case of choked jets the energy fluence may be enhanced by $f_b^{-1}\sim 100$, and the detection of GeV neutrinos becomes possible even for extragalactic SNe out to ~ 1 Mpc.

HK has the fiducial volume of 0.56 Mt, so the effective numbers of free protons and bounded nucleons in oxygens are 3.7×10^{34} and 3.0×10^{35}, respectively. The neutrino-nucleon cross section for the charged-current interaction at 1 GeV is $\sim 0.6\times10^{-38}~{\rm cm}^2$ (averaged over ν and $\bar{\nu}$), so the effective area is $\sim 2\times10^{-3}~{\rm cm}^2$. Hence, we may expect $\sim 70~\mathcal{E}_{\nu,48}^{\rm iso}$ events for a SN at 10 kpc. In addition, HK could also allow us to see $\sim 10-100$ MeV neutrinos, through the $\bar{\nu}_e p \rightarrow e^+ n$ channel. But the detection would be more difficult due to smaller cross sections at lower energies and the signal may be buried in the exponential tail of thermal MeV neutrinos from the PNS.

To see the signal, it is crucial to reduce backgrounds using space/time-coincidence. The obvious background is the atmospheric neutrino background (ANB). The ANB at GeV is $\approx 1.3\times10^{-2}~{\rm GeV~cm^{-2}~s^{-1}~sr^{-1}}$ for $\nu_e+\bar{\nu}_e$ and $\approx 2.6\times10^{-2}~{\rm GeV~cm^{-2}~s^{-1}~sr^{-1}}$ for $\nu_\mu+\bar{\nu}_\mu$, respectively [27]. We may take the time window of $t_{\rm thin}\sim 10-100$ s after the explosion time that is measurable with MeV neutrinos and/or gravitational waves [28]. The localization is possible by optical follow-up observations, and the angular resolution of PINGU is expected to be $\sim 2-20$ deg [15]. Then, the ANB in this time and angular window, $\sim 2\times10^{-3}~{\rm erg~cm^{-2}}$, is negligible.

Implications and discussions.— Neutron-loaded relativistic winds emanate from rotating and magnetized PNSs during their $\sim 10-100$ s cooling epoch. Relativistic neutrons produce $\sim 0.1-1$ GeV neutrinos via the np reaction as the wind/jet-driven bubble interacts with the surrounding stellar material. For PNSs with $B_{\rm dip}\gtrsim 10^{14}$ G and $P\sim 1-10$ ms, future neutrino telescopes such as PINGU and HK may detect $\sim 10-100$ neutrino events of energy $\sim 0.1-1$ GeV from the next Galactic SN. Even extragalactic SNe may be detected if the wind is collimated, forming choked jets. Although not all SNe are born with such high $B_{\rm dip}$ and short P, $\gtrsim 10\%$ of SNe may be [7], and we may expect $0.02-0.05~{\rm yr}^{-1}$ for the birth of magnetars within 5 Mpc [29]. In addition, given the ANB is reduced by coincident detections and follow-up observations, stacking analyses for nearby SNe could be useful (c.f. GRBs [31]).

The detection of quasi-thermal neutrinos would prove the existence of relativistic neutron outflows, which cannot be probed by photon observations. We could get precious insights into magnetic acceleration mechanisms, the physics of PNSs, and clues to nucleosynthesis. Multi-wavelength studies at radio, optical and x-rays are also relevant to test our picture and constrain $B_{\rm dip}$ and P. Detecting these neutrinos would also be useful in revealing the SN-GRB connection. Indeed, rapidly-rotating and strongly-magnetized PNSs have been proposed as the central engine of successful jets leading to GRBs in compact stellar progenitors. A larger fraction of PNSs would have less extreme $B_{\rm dip}$ and P, leading to failed GRBs, hypernovae and perhaps super-luminous SNe.

Importantly, quasi-thermal neutrinos, which we have discussed, do not require uncertain cosmic-ray ion acceleration mechanisms, leading to non-thermal, high-energy neutrinos [29, 30]. For example, wakefield-like acceleration in the PNS wind could generate UHECRs and resulting PeV-EeV neutrinos via interactions with the stellar material and SN photons [29]. Note that mechanisms producing those neutrinos are completely different, which may occur only at $t\gg t_{\rm thin}$ (where $\dot{M}\approx\dot{M}_{\rm GJ}$).

The optical depth for the νN interaction is small. The near-spherical wind interacts with the shocked stellar material, and we have $\sim 0.1(M_{\rm sn}/10M_\odot)R_{\rm sn,10}^{-2}$ at GeV, where $R_{\rm sn}$ is the SN ejecta radius. The jet may interact with the pre-shocked envelope, and we have only $\sim 10^{-4}$ at GeV if $\rho\sim 1~{\rm g~cm^{-3}}$ at $10^{10.5}$ cm. However, studying neutrino oscillations in the MeV-GeV range may be interesting. For example, the matter effect is relevant since the resonance happens at $\approx 0.22~{\rm g~cm^{-3}}~(E_\nu/{\rm GeV})^{-1}(\Delta m^2/7.59\times10^{-5}~{\rm eV}^2)$, and we can use it to probe the density profile or check neutrino properties given the progenitor structure (c.f. [32, 33]).

Acknowledgments.— We thank John Beacom, Kumiko Kotera, Peter Mészáros, Brian Metzger, especially Masayuki Nakahata and Carsten Rott for helpful comments, and the support by CCAPP workshop, Revealing Deaths of Massive Stars with GeV-TeV Neutrinos.

---

[1] A. Burrows and J. M. Lattimer, Astrophys. J. **307**, 178 (1986).
[2] J. A. Pons *et al.*, Astrophys. J. **513**,780 (1999).
[3] S. E. Woosley *et al.*, Astrophys. J. **433**, 209 (1994).

[4] Y.-Z. Qian and S. E. Woosley, Astrophys. J. **471**, 331 (1996).

[5] T. A. Thompson, P. Chang, and E. Quataert, Astrophys. J. **611**, 380 (2004).

[6] B. D. Metzger *et al.*, Mon. Not. R. Astron. Soc. **413**, 2031 (2011).

[7] P. M. Woods and C. Thompson, Compact Stellar X-ray Sources, edited by W. H. G. Lewin and M. van der Klis, Cambridge Astrophysics Series Vol. 39 (2006), p. 547; S. Mereghetti, Astron. Astrophys. Rev. **15**, 225 (2008).

[8] R. C. Duncan and C. Thompson, Astrophys. J. **392**, 9 (1992); C. Thompson and R.C. Duncan, Astrophys. J. **408**, 194 (1993).

[9] N. Bucciantini *et al.*, Mon. Not. R. Astron. Soc. **380**, 1541 (2007); **396**, 2038 (2009).

[10] S. S. Komissarov and M. V. Barkov, Mon. Not. R. Astron. Soc. **382**, 1029 (2007).

[11] V. Usov, Nature **357**, 472 (1994).

[12] J. C. Wheeler, I. Yi, P. Höflich, and L. Wang, Astrophys. J. **537**, 810 (2000); D. Kasen and L. Bildsten, Astrophys. J. **717**, 245 (2010).

[13] F. C. Michel, Astrophys. J. **158**, 727 (1969).

[14] B. D. Metzger, D. Giannios, and S. Horiuchi, Mon. Not. R. Astron. Soc. **415**, 2495 (2011); S. Horiuchi *et al.*, Astrophys. J. **753**, 69 (2012).

[15] D. J. Koskinen, Mod. Phys. Lett. A **26**, 2899 (2011); K. Clark and D. F. Cowen, Nucl. Phys. B Proc. Suppl. **00**, 1 (2012).

[16] K. Abe *et al.*, arXiv:1109.3262 (2011).

[17] T. A. Thompson, E. Quataert, and A. Burrows, Astrophys. J. **620**, 861 (2005).

[18] B. D. Metzger, T. A. Thompson, and E. Quataert, Astrophys. J. **676**, 1130 (2008).

[19] P. Goldreich and W. H. Julian, Astrophys. J. **157**, 869 (1969).

[20] P. Goldreich and W. H. Julian, Astrophys. J. **160**, 971 (1970).

[21] S. S. Komissarov, Mem. della Soc. Astron. Italiana **82**, 95 (2011).

[22] H. C. Spruit, F. Daigne, and G. Drenkahn, Astrophys. Astron. **369**, 694 (2001); G. Drenkann, Astrophys. Astron. **387**, 714 (2002).

[23] A. Beresnyak, arXiv:1301.7424.

[24] E. Waxman and P. Mészáros, Astrophys. J. **584**, 390 (2003).

[25] J. N. Bahcall and P. Mészáros, Phys. Rev. Lett. **85**, 1362 (2000); P. Mészáros and M. J. Rees, Astrophys. J. **733** L40 (2011).

[26] J. P. Rachen, Ph. D Thesis (1996).

[27] M. Honda, T. Kajita, K. Kasahara and S. Midorikawa, Phys. Rev. D **83**, 123001 (2011).

[28] I. Bartos, P. Brady, and S. Márka, arXiv:1212.2289.

[29] K. Murase, P. Mészáros, and B. Zhang, Phys. Rev. D **79**, 103001 (2009).

[30] T. K. Gaisser and T. Stanev, Phys. Rev. Lett. **58**, 1695 (1987); W. Bednarek and R. J. Protheroe, Phys. Rev. Lett. **79**, 2616 (1997); J. H. Beall and W. Bednarek, Astrophys. J. **569**, 343 (2002).

[31] K. Murase, K. Kashiyama, and P. Mészáros, arXiv:1301.4236 ; I. Bartos, A. M. Beloborodov, K. Hurley, and S. Márka, arXiv:1301.4232.

[32] R. C. Schirato and G. M. Fuller, arXiv:astro-ph/0205390.

[33] K. Takahashi, K. Sato, A. Burrows, and T. A. Thompson, Phys. Rev. D **68**, 113009 (2003).